Evaluation of Nucleoside Hydrolase Inhibitors for Treatment of African Trypanosomiasis[▽][†]

Maya Berg,[1] Linda Kohl,[2] Pieter Van der Veken,[1] Jurgen Joossens,[1] Mohammed I. Al-Salabi,[3]
Valeria Castagna,[4] Francesca Giannese,[4] Paul Cos,[5] Wim Versées,[6] Jan Steyaert,[6] Philippe Grellier,[2]
Achiel Haemers,[1] Massimo Degano,[4] Louis Maes,[5] Harry P. de Koning,[3] and Koen Augustyns[1]*

*Laboratory of Medicinal Chemistry, University of Antwerp, Universiteitsplein 1, B-2610 Antwerp, Belgium[1]; Muséum National d'Histoire
Naturelle, USM 504-EA3335, Biologie Fonctionnelle des Protozoaires, 61 Rue Buffon, CP52, Paris Cedex 05 75231, France[2];
Institute of Biomedical and Life Sciences, Division of Infection and Immunity, Glasgow Biomedical Research Centre,
University of Glasgow, 120 University Place, Glasgow G12 8TA, United Kingdom[3]; Biocrystallography Unit and
Mass Spectrometry Unit, DIBIT San Raffaele Scientific Institute, via Olgettina 58, 20132 Milan, Italy[4];
Laboratory of Microbiology, Parasitology and Hygiene, University of Antwerp, Groenenborgerlaan 171,
B-2020 Antwerp, Belgium[5]; and Structural Biology Brussels, Vrije Unversiteit Brussel, and
Department of Molecular and Cellular Interactions, VIB, Pleinlaan 2, B-1050 Brussels, Belgium[6]*

In this paper, we present the biochemical and biological evaluation of *N*-arylmethyl-substituted iminoribitol derivatives as potential chemotherapeutic agents against trypanosomiasis. Previously, a library of 52 compounds was designed and synthesized as potent and selective inhibitors of *Trypanosoma vivax* inosine-adenosine-guanosine nucleoside hydrolase (IAG-NH). However, when the compounds were tested against bloodstream-form *Trypanosoma brucei brucei*, only one inhibitor, *N*-(9-deaza-adenin-9-yl)methyl-1,4-dideoxy-1,4-imino-D-ribitol (UAMC-00363), displayed significant activity (mean 50% inhibitory concentration [IC_{50}] ± standard error, 0.49 ± 0.31 μM). Validation in an *in vivo* model of African trypanosomiasis showed promising results for this compound. Several experiments were performed to investigate why only UAMC-00363 showed antiparasitic activity. First, the compound library was screened against *T. b. brucei* IAG-NH and inosine-guanosine nucleoside hydrolase (IG-NH) to confirm the previously demonstrated inhibitory effects of the compounds on *T. vivax* IAG-NH. Second, to verify the uptake of these compounds by *T. b. brucei*, their affinities for the nucleoside P1 and nucleoside/nucleobase P2 transporters of *T. b. brucei* were tested. Only UAMC-00363 displayed significant affinity for the P2 transporter. It was also shown that UAMC-00363 is concentrated in the cell via at least one additional transporter, since P2 knockout mutants of *T. b. brucei* displayed no resistance to the compound. Consequently, no cross-resistance to the diamidine or the melaminophenyl arsenical classes of trypanocides is expected. Third, three enzymes of the purine salvage pathway of procyclic *T. b. brucei* (IAG-NH, IG-NH, and methylthioadenosine phosphorylase [MTAP]) were investigated using RNA interference. The findings from all these studies showed that it is probably not sufficient to target only the nucleoside hydrolase activity to block the purine salvage pathway of *T. b. brucei* and that, therefore, it is possible that UAMC-00363 acts on an additional target.

In the search for new selective trypanocidal drugs, it has been proposed that the purine metabolism of *Trypanosoma brucei* provides a valuable target. In contrast to mammals, all parasites are unable to synthesize purines *de novo* and rely instead on the purine salvage pathway (PSP) to obtain purines, which are essential for their survival. The PSP is essential for all stages of *T. brucei*. The following enzymes of the PSP in *T. brucei brucei* are described in the literature (Fig. 1): inosine-adenosine-guanosine nucleoside hydrolase (IAG-NH; EC.3.2.2.1) (33, 38), inosine-guanosine nucleoside hydrolase (IG-NH; EC 3.2.2.1) (32), methylthioadenosine phosphorylase (MTAP; EC 2.4.2.28) (43), adenine phosphoribosyltransferase (APRT; EC 2.4.2.7) (5), hypo-

xanthine-guanine phosphoribosyltransferase (HGPRT; EC 2.4.2.8) (36), and adenosine kinase (AK; EC 2.7.1.20) (5). Key enzymes in the PSP of *T. brucei* are the nucleoside hydrolases (NH; EC 3.2.2.1). In these parasites, purine bases are obtained by cleavage of the N-glycosidic bond of nucleosides by NH. In *T. b. brucei*, two types of NH are present: the purine nucleoside-specific IAG-NH, which prefers inosine, adenosine, and guanosine as substrates, and the 6-oxopurine-specific IG-NH, with high affinities for inosine and guanosine (30, 32, 38). It should be noted that NH activity is absent in mammalian cells. Therefore, NH may provide a good target for the development of new antitrypanosomal compounds (19). Consequently, this target has been investigated during the past decade, and potent inhibitors of NH have been developed. The immucillins (20, 29) and *N*-arylmethyl-substituted iminoribitol derivatives (4, 22, 23, 39) (Fig. 2) are the strongest inhibitors of *T. vivax* IAG-NH (TvIAG-NH) and *T. b. brucei* IAG-NH (TbbIAG-NH) known to date, with K_i values in the low nanomolar range. Additionally, many of these inhibitors show selectivity with respect to the human nucleoside-cleaving enzyme human pu-
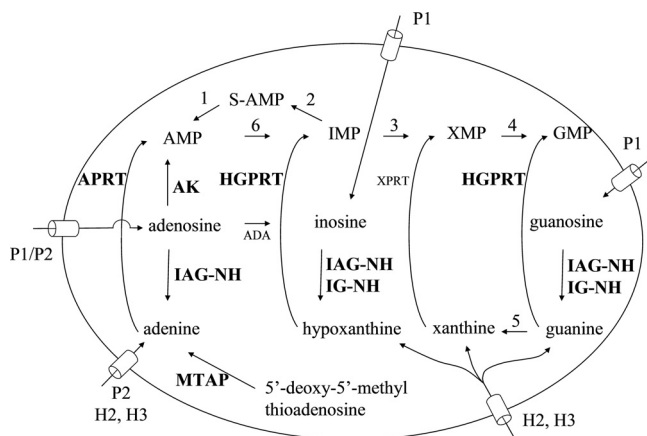
FIG. 1. PSP of *T. brucei* depicted with key enzymes and transporters. 1, S-AMP lyase; 2, S-AMP synthetase; 3, IMP dehydrogenase; 4, GMP synthetase; 5, guanine deaminase; 6, AMP deaminase.

FIG. 2. Structures of immucillins and *N*-arylmethyl-substituted iminoribitols. OMe, OCH$_3$.

rine nucleoside phosphorylase (hPNP) (4). So far, no data on the activities of these classes of inhibitors against *T. b. brucei* have been published. We hereby reveal the activities of the *N*-arylmethyl-substituted iminoribitol derivatives against *T. b. brucei*. Interestingly, only 1 compound in a series of 52 compounds (see the supplemental material) shows remarkable activity *in vitro* against bloodstream-form (BSF) *T. b. brucei* and *T. b. rhodesiense*. This activity was confirmed in an *in vivo* model of African trypanosomiasis. The lack of activity of all other compounds may be due to several factors. First, since enzymatic screening was performed with TvIAG-NH, as this enzyme was easily accessible at the time, differences between the NH enzymes of *T. vivax* and *T. b. brucei* may be the cause of the lack of observed biological activity against *T. b. brucei*. The percent sequence identity of the IAG-NH proteins from the orthologous organisms *T. vivax*, *T. b. brucei*, *T. congolense*, and *Leishmania major* was determined by a shotgun alignment study using Mac Molly Tetra software. The amino acid sequence of IAG-NH from *T. vivax* showed 68% sequence identity to the protein from *T. b. brucei*, 64% to the protein from *T. congolense*, and 56% to the protein from *L. major*. Second, the absence of antiprotozoal activity may be a reflection of difficulties with uptake of the compounds. All protozoan parasites studied to date are auxotrophic for purines and depend on the transport of various natural nucleosides and nucleobases (12). For *T. brucei*, the multiplicity of transporters is puzzling, and it remains unclear why this unicellular parasite requires so many. Examination of the *T. brucei* genome revealed genes for 12 distinct equilibrative nucleoside transporter (ENT) family members, most of which have now been shown to be involved in the uptake of nucleosides and/or nucleobases (31). *N*-Aryl-methyl-substituted iminoribitol derivatives may be transported into the cell via P1 and P2 transporters (Fig. 1). *T. brucei AT1* (Tb*AT1*), the first ENT gene to be identified in trypanosomes, encodes the P2 adenosine/adenine transporter (27). In addition to fulfilling a role in purine salvage, this gene product has been shown to be the main transporter for the melaminophenyl arsenicals (e.g., melarsoprol) and diamidine drugs (e.g., pentamidine) that constitute the first-line treatment for trypanosomiasis (7, 28). This transporter is ex-
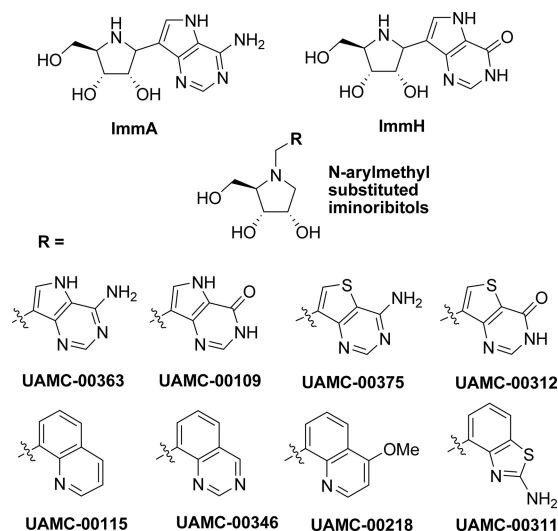
pressed only in BSF parasites (16). A cluster of genes on chromosome 2, *T. brucei NT2* (Tb*NT2*) to Tb*NT7*, encode a number of purine nucleoside transporters, collectively known as P1 transporters, several of which are expressed in BSFs (35). They mediate the uptake of adenosine, inosine, guanosine, and in some cases hypoxanthine (7, 16, 35). Genes for two additional P1-type transporters, designated TbNT10/AT-B and TbNT9/AT-D, are located on chromosomes 6 and 9 (2). Third, the target enzyme NH may not be crucial for the survival of the parasite because of the existence of bypass mechanisms in the PSP (Fig. 1). To investigate these different hypotheses, several experiments were performed. The most potent compounds of the library (Fig. 2) were screened against TbbIAG-NH and *T. b. brucei* IG-NH (TbbIG-NH) to confirm the previously demonstrated inhibitory effects of the compounds on TvIAG-NH. A set of transporter studies was also performed. Uptake of these compounds was verified by measurement of affinities for the nucleoside P1 and nucleoside/nucleobase P2 transporters of *T. b. brucei*. In order to examine the importance of the purine salvage enzymes for growth and survival of procyclic *T. b. brucei*, the expression of a set of enzymes (IAG-NH, IG-NH, and MTAP) was knocked down by RNA interference (RNAi).

MATERIALS AND METHODS

Synthesis of *N*-(9-deaza-adenin-9-yl)methyl-1,4-dideoxy-1,4-imino-D-ribitol (UAMC-00363). The synthesis of compound UAMC-00363 has been described previously (22), but minor changes in the last reaction step and purification were made: iminoribitol · HCl (0.15 g [0.887 mmol]), sodium acetate (NaOAc; 0.08 g [0.975 mmol]), and 37% aqueous formaldehyde (0.073 ml [0.975 mmol]) were dissolved in H$_2$O-dioxane (4:1 [2 ml/mmol]). The reaction mixture was stirred at 95°C for 1.5 h. 9-Deazaadenine (0.242 g [0.975 mmol]) was added to the solution, and the mixture was stirred at 95°C for an additional hour. After cooling down to room temperature, the crude mixture was converted to its HCl salt with 1 N HCl. Excess HCl was removed by evaporation under reduced pressure, and the crude mixture was adsorbed onto silica gel, which was then evaporated to dryness under reduced pressure. Purification by column chromatography (dichloromethane/methanol/NH$_4$OH ratio, 80:20:1 to 80:20:5) yielded the product, which was again converted to its HCl salt (0.045 g [15%]). Nuclear magnetic resonance

data, mass measurements, and high-performance liquid chromatography (HPLC) data can be found in the supplemental material.

Enzyme inhibition studies. (i) TvIAG-NH. Details of the TvIAG-NH inhibition assay and experimental determination of inhibitor constants (K_i values) have been given previously (22).

(ii) TbbIAG-NH and TbbIG-NH. TbbIAG-NH and TbbIG-NH assays were performed with recombinant, purified enzymes (details are to be published elsewhere). All measurements were carried out at 37°C in 50 mM HEPES, pH 7.3. The $\Delta\varepsilon$ values (difference in molar absorption between the product [free base] and substrate [nucleotide] at the indicated wavelength) used were −4.0 mM^{-1} · cm^{-1} at 260 nm for guanosine and −0.82 mM^{-1} · cm^{-1} at 280 nm for inosine. Progress curves were recorded with an Ultrospec 2100 spectrophotometer (GE Healthcare). For the IG-NH enzyme, the K_i values of the compounds were determined by measuring the initial velocities for the enzymatic hydrolysis of a fixed guanosine concentration nearing the Michaelis constant (K_m) with at least three inhibitor concentrations. Competitive inhibition was assumed based on the similarity between the substrate and the inhibitor. Experimental data were fitted to the following equation:

$$\frac{v_I}{v_o} = \frac{K_m + [S]}{K_m \left(1 + \dfrac{[I]}{K_i}\right) + [S]}$$

where v_I and v_o represent the initial reaction rates in the presence and absence of the inhibitor and $[S]$ and $[I]$ are the substrate and inhibitor concentrations, respectively. For the IAG-NH enzyme, inosine was used as the substrate and inhibitor constants were determined by a full kinetic analysis measuring the apparent Michaelis constant (K_m^*) in the presence of a fixed inhibitor concentration. Initial velocities measured at different substrate concentrations were fitted to the Michaelis-Menten equation by using the program Prism (GraphPad Software, Inc.). Inhibitor constants were calculated with the following equation for competitive inhibition:

$$K_m^* = K_m \cdot \left(1 + \frac{[I]}{K_i}\right)$$

(iii) hPNP. Details of the hPNP assay and experimental determination of K_i values have been given elsewhere (4).

Quantification of in vitro antiparasitic activity. The *T. b. brucei* Lister 427 strain (suramin sensitive) or *T. b. rhodesiense* (strain STIB-900) was used for screening at the University of Antwerp (UA). The strains were maintained in Hirumi (HMI-9) medium supplemented with 10% inactivated fetal calf serum. All cultures and assays were conducted at 37°C under an atmosphere of 5% CO$_2$. Assays were performed with sterile 96-well microtiter plates, each well containing 200 μl of medium with 1.5×10^4 parasites/well and the test compound at the appropriate dilution. Compounds were tested at five concentrations (64, 16, 4, 1, and 0.25 μM or mg/ml). Parasite growth was compared to that in untreated infected control medium (100% parasite growth) and that in uninfected control medium (0% growth). After 3 days of incubation, parasite growth was assessed fluorimetrically after the addition of 50 μl resazurin (Alamar blue; 10 μg/ml) per well. After 15 h (for *T. b. rhodesiense*) or 24 h (for *T. b. brucei*) at 37°C, fluorescence was measured (excitation λ, 550 nm; emission λ, 590 nm). The results were expressed as the percent reduction in parasite growth/viability compared to that in control wells, and a 50% inhibitory concentration (IC$_{50}$) was calculated. When the IC$_{50}$ was <1 μM, a secondary screening with *T. b. brucei* and *T. b. rhodesiense* was performed and IC$_{50}$s were determined using an extended dose range (2-fold compound dilutions). Compounds were also tested against a nifurtimox-sensitive *T. cruzi* Tulahuen CL2 β-galactosidase strain, *Leishmania infantum* MHOM/MA/67/ITMAP263 intracellular amastigotes, and a chloroquine-sensitive (Ghana) strain of *Plasmodium falciparum* (ring stages and schizonts). Suramin, melarsoprol, nifurtimox, miltefosine, and chloroquine, respectively, were included as the reference drugs. Cytotoxicity was tested with human simian virus 40-immortalized lung fibroblasts (MRC-5 SV2 cells; European Collection of Cell Cultures, United Kingdom) (11). IC$_{50}$s were also obtained at the University of Glasgow (UG) using a very similar protocol, with essentially identical results. Minor differences in the protocol included an incubation time of 48 h in the presence of 2-fold dilutions of the test compound, starting at a concentration of 100 μM, followed by further incubation for 24 h in the presence of resazurin (Alamar blue [12.5 μg/ml; Sigma]). The UG experiments, like those at UA, used *T. b. brucei* strain 427 as the standard drug-sensitive control, assayed in parallel with the TbAT1 knockout (TbAT1-KO) (28) and B48 (6) drug-resistant strains. Diminazene aceturate and pentamidine (both from Sigma) were used as positive controls for the resistance phenotypes.

Real-time assay for trypanosome viability and mobility. The assay for trypanosome viability and mobility was performed exactly as described previously (6). The curves of trypanosome inhibition were determined by absorption at 750 nm using a UV/visible spectrophotometer (HP-8453; Hewlett Packard). Cultured *T. b. brucei* BSFs of strain 427 were used at a density of 10^7 cells per ml in HMI-9 medium. Phenylarsine oxide (Sigma) was used as a positive control.

In vivo assay. Female Swiss Webster mice (4/group) were treated orally with UAMC-00363 at 50 mg/kg of body weight and, 1 h later, were intraperitoneally (i.p.) infected with 10^4 trypanosomal BSFs (*T. b. brucei* Lister strain 427), collected from an infected donor animal, in a volume of 0.25 ml per mouse. i.p. treatment at 50 mg/kg was continued for the next 4 days. The reference compound suramin (administered i.p. at 10 mg/kg/day) was included. Untreated infected controls generally die between 6 days postinfection (dpi) and 9 dpi. To obtain information about the parasitemia of survivors, on days 10, 14, and 21 postinfection, 10 μl of blood was obtained from the tail vein for microscopic estimation of the level of parasitemia. The animals were observed for the occurrence/presence of clinical and adverse effects during the course of the experiment. The occurrence of mortality was monitored daily.

Transport studies. Analyses of the transport of [^{3}H]adenosine (Amersham; 23 Ci/mmol) and [^{3}H]hypoxanthine (Amersham; 19 Ci/mmol) were performed exactly as described previously (2, 40). Briefly, *T. b. brucei* strain 427 BSFs were collected from infected Wistar rats at peak parasitemia by cardiac puncture under terminal anesthesia and separated from blood cells on a DEAE-52 anion exchange column (Whatman). Trypanosomes were washed twice with assay buffer (33 mM HEPES, 98 mM NaCl, 4.6 mM KCl, 0.55 mM CaCl$_2$, 0.07 mM MgSO$_4$, 5.8 mM NaH$_2$PO$_4$, 0.3 mM MgCl$_2$, 23 mM NaHCO$_3$, and 14 mM glucose, pH 7.3) and resuspended in the same buffer at a concentration of 2×10^8/ml. Aliquots of 100 μl of this suspension were incubated for 30 s with the same volume of radiolabel at room temperature in the presence or absence of test compounds. Incubations were ended by the addition of 1 ml ice-cold unlabeled 1 mM adenosine (for P1 or P2) or hypoxanthine (for H2) and immediate centrifugation through an oil layer. Radioactivity was determined using a scintillation counter. K_i values were calculated by nonlinear regression using the Prism 4 and 5 software packages (GraphPad) and the Cheng-Prusoff equation: $K_i = IC_{50}/(1 + [L]/K_m)$, in which $[L]$ is the permeant concentration used and K_m is the Michaelis constant for the transporter-permeant combination (8).

RNAi knockdown studies. (i) Trypanosome cell lines and cultures. All cell lines were derivatives of *T. b. brucei* strain 427 and were cultured in SDM79 (42) medium with hemin and 10% fetal calf serum. *T. brucei* 29-13 procyclic cells that express T7 RNA polymerase and a tetracycline repressor (42) were transformed with the pZJM vector expressing double-stranded RNA from two tetracycline-inducible T7 promoters facing each other (41), yielding cell lines with RNAi knockdown of TbIAG-NH, TbIG-NH, TbMTAP, and all three enzymes together (TbIAG-NH^{RNAi}, TbIG-NH^{RNAi}, TbMTAP^{RNAi}, and TbMTAP-IAGNH-IGNH^{RNAi} cells, respectively). The plasmid was introduced into 29-13 cells by electroporation, and resistant clones were selected by the addition of selection medium (15 μg/ml G418, 20 μg/ml hygromycin, 2 μg/ml phleomycin). RNAi was induced by the addition of 1 μg tetracycline per ml of medium, and fresh tetracycline was added at each cell dilution. The GeneDB database was searched for IAG-NH, IG-NH, and MTAP genes. Primer sequences were designed using *RNAit* primer design software, available at the TrypanoFAN website (http://trypanofan.path.cam.ac.uk/software /RNAit.html). Primer sequences are available upon request.

(ii) RT-PCR. Total RNA was extracted from cells grown with or without tetracycline for 48 h, and reverse transcription-PCR (RT-PCR) was performed as described by Absalon et al. (1).

(iii) Fluorescence assay. The fluorescence assay was performed as described previously (1). Slides were observed with a Leica digital module R (DMR) microscope, and images were captured with a Cool Snap HQ camera (Roper Scientific).

RESULTS

Enzyme assays. The design and synthesis of the *N*-aryl-methyl-substituted iminoribitol derivatives has been discussed extensively elsewhere (4, 22, 23). These compounds are potent inhibitors of TvIAG-NH and discriminate against hPNP (Table 1). Since biological assays were performed with a *T. b. brucei* strain, compounds (Fig. 2) were screened against TbbIAG-NH to confirm the inhibitory effect (Table 1). All compounds are nanomolar inhibitors of the enzyme. The most

TABLE 1. Biochemical and biological activities of immucillins and *N*-arylmethyl-substituted iminoribitols[a]

Compound	K_i (μM) for				IC_{50} (μM) for:	
	TvIAG-NH	TbbIAG-NH	TbbIG-NH	hPNP	*T. b. brucei*	MRC-5 SV2 cells
ImmA	$(6.2 \pm 0.3) \times 10^{-3}$	0.9×10^{-3}*	$(4.4 \pm 0.9) \times 10^{-3}$	>10*	>64	>64
ImmH	$(6.2 \pm 0.7) \times 10^{-3}$	24×10^{-3}*	$(9 \pm 2) \times 10^{-3}$	$(0.056 \pm 0.015) \times 10^{-3}$*	>64	>64
UAMC-00363	$(4.1 \pm 0.7) \times 10^{-3}$	$(18 \pm 2) \times 10^{-3}$	32 ± 5	22.5 ± 5.5	0.49 ± 0.31[b]	>64
UAMC-00109	$(4.4 \pm 0.5) \times 10^{-3}$	$(30 \pm 3) \times 10^{-3}$	138 ± 40	$(5.8 \pm 1.5) \times 10^{-3}$	>64	>64
UAMC-00375	$(19 \pm 4) \times 10^{-3}$	$(56 \pm 6) \times 10^{-3}$	31 ± 5	$>10^3$	>64	>64
UAMC-00312	$(20 \pm 3) \times 10^{-3}$	$(190 \pm 20) \times 10^{-3}$	120 ± 27	77.6 ± 18.8	34	>64
UAMC-00115	$(11 \pm 1) \times 10^{-3}$	$(446 \pm 36) \times 10^{-3}$	11 ± 2	$>10^3$	>64	>64
UAMC-00346	$(58 \pm 10) \times 10^{-3}$	ND	ND	$>10^3$	>64	>64
UAMC-00218	$(29 \pm 6) \times 10^{-3}$	ND	ND	$>10^3$	>64	>64
UAMC-00311	$(40 \pm 6) \times 10^{-3}$	$(560 \pm 55) \times 10^{-3}$	14 ± 2	$>10^3$	>64	>64

[a] Inhibition of TvIAG-NH (4, 22, 37), TbbIAG-NH (21, 29), TbbIG-NH, and hPNP (4, 21, 24) (indicated by K_i values) and inhibition of *T. b. brucei* (indicated by IC_{50}s). Cytotoxicity (expressed as the IC_{50}) was measured with human fibroblasts (MRC-5 SV2 cells). For K_i values, standard errors on the fit are provided. *, K_i* for slow-onset inhibition; ND, not determined.
[b] The data shown are the averages of results from eight independent determinations.

potent compounds were UAMC-00363 (K_i = 18 nM) and UAMC-00109 (K_i = 30 nM), bearing a hydrophobic aglycone that mimics purine nucleoside substrates adenosine and inosine, respectively. Replacing the deazapurine moiety by thienopyrimidine lowered the efficacy of the inhibitors, as judged from the increase in the K_i values to 56 nM (for UAMC-00375) and 190 nM (for UAMC-00312). The efficacy of inhibition further decreased when the purine ring was replaced by an aminobenzothiazole ring (yielding UAMC-00311; K_i = 560 nM) or a quinoline ring (yielding UAMC-00115; K_i = 446 nM). Taken together, these results suggest that, with respect to the aglycone part, structure-activity relationships for TbbIAG-NH inhibition seem to differ substantially from what was observed earlier for TvIAG-NH (4, 22). The same set of compounds was also tested with TbbIG-NH. Surprisingly, the inhibition of this enzyme was less efficient than that of IAG-NH, with K_i values in the micromolar range. For IG-NH, the most efficient compounds were the quinoline derivative UAMC-00115 (K_i = 11 μM) and UAMC-00311 (K_i = 14 μM). The activities of the adenosine-mimicking UAMC-00363 (K_i = 32 μM) and its analogue UAMC-00375 (K_i = 31 μM) were 3-fold lower. The inhibitory activities of inosine mimics UAMC-00109 (K_i = 138 μM) and UAMC-00312 (K_i = 120 μM) were 10-fold lower. Thus, the IAG-NH and IG-NH enzymes clearly differ in the active site features, allowing isozyme-selective inhibition. The fact that TbbIG-NH remained unaffected and hence fully functional in the PSP (Fig. 1) may be a first indication for the observed lack of antiparasitic activity. It will be of interest to experimentally identify the active site features that influence the affinities of IAG-NH and IG-NH for the compounds tested here.

***In vitro* activity against *T. b. brucei*.** Nearly all of the 52 compounds (see the supplemental material) were tested *in vitro* against *T. b. brucei* (strain 427 BSFs). Most compounds did not display IC_{50}s below 5 μM and, accordingly, were considered to be inactive against this parasite. Additionally, no activity against *T. cruzi*, *L. infantum*, or *P. falciparum* was found. Only one compound, UAMC-00363, showed high-level and selective activity against *T. b. brucei* (mean IC_{50} ± standard error = 0.49 ± 0.31 μM) in the absence of cytotoxicity to a human cell line (Table 1). In a secondary

screening, this compound also showed activity against *T. b. rhodesiense* (IC_{50} = 0.26 ± 0.15 μM). This compound was further tested in a mouse model of African trypanosomiasis.

A deeper investigation of the trypanostatic and trypanocidal mode of action of UAMC-00363 was performed. The compound was relatively slow acting, apparently inducing growth arrest and becoming trypanocidal only at high concentrations (>5 μM). This was apparent from the biphasic inhibition curve displayed in the Alamar blue assay (Fig. 3A), similar to the previously defined curve for the trypanostatic adenosine analogue NA-42, where the first IC_{50} corresponds to the concentration inducing growth arrest and the second IC_{50} corresponds to the concentration inducing a parasitocidal effect (34). We thus examined the rate at which trypanosomes are killed by UAMC-00363 by using an *in vitro* lysis assay as described previously, with phenylarsine oxide as a positive control (28). Figure 3B shows that the test compound at concentrations up to 20 μM failed to affect trypanosome viability or motility for over 7 h. Cells were thus monitored by microscopic counting for a 48-h period (Fig. 3C). Phenylarsine oxide (0.25 μM) killed all cells within 5 h, whereas pentamidine (1 μM) took 24 h. Yet incubation with 10 μM UAMC-00363 reduced the trypanosome population by approximately 75% after 48 h; no trypanocidal effect was observed at 24 h (Fig. 3C). To test whether continuous exposure is required for the trypanostatic effect, parallel cultures of *T. b. brucei* were exposed to pentamidine or UAMC-00363 for only 5 h, after which they were washed in fresh medium without a test compound. In both cases, the drug effect was only slightly reversed after removal of the drug (Fig. 3C).

***In vivo* assay.** UAMC-00363 at a dose of 50 mg/kg was assessed in a rodent model of *T. b. brucei* infection. The vehicle-infected controls developed severe trypanosomiasis with 100% mortality at 9 dpi. Treatment with suramin at 10 mg/kg i.p. for 5 days resulted in 100% survival at 21 dpi with total clearance of parasitemia at 10 dpi. Treatment with compound UAMC-00363 at 50 mg/kg once daily for 5 days (the dose on day 1 was given orally, and i.p. treatment was administered for the next 4 days) totally cleared the infection, as reflected by parasite-negative blood samples obtained at 10, 14, and 21 dpi, and resulted in 75% survival at 21 dpi (Fig. 4). Additional
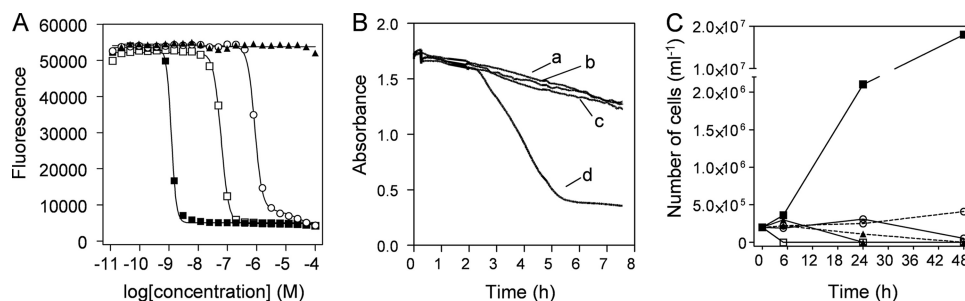
FIG. 3. Effect of UAMC-00363 on *T. b. brucei* cultures. (A) Results of the Alamar blue assay with *T. b. brucei* strain 427. ○, UAMC-00363; ▲, UAMC-00109; ■, pentamidine; □, diminazene aceturate. Data are expressed as relative fluorescence units. (B) Effects of UAMC-00363 on the viability and motility of *T. b. brucei*. Trypanosomes (10^7 in 1 ml assay buffer) were placed in a cuvette, and absorbance at 750 nm was measured for approximately 7.5 h. The assay is based on light scatter by the highly mobile flagellated trypanosomes; reduction in either cell viability or motility will thus reduce absorbance. (a) Negative control (no test compound added); (b) UAMC-00363 at 20 μM; (c) UAMC-00363 at 10 μM; (d) positive control (phenylarsine oxide at 1 μM). (C) Cultures of 2×10^5 BSF *T. b. brucei* parasites of strain 427 were incubated with 0.25 μM phenylarsine oxide (□), 1 μM pentamidine (▲), 10 μM UAMC-00363 (○), or no test compound (control; ■) for up to 48 h (solid lines) or for only 5 h, after which the drug was washed out by centrifugation (twice) and the cells were resuspended in fresh medium (dashed lines). Cell counts were determined in duplicate with a hemocytometer under a phase-contrast microscope; average counts are shown.

experiments are planned to further explore this promising activity.

Transport studies. In order to examine the lack of antiprotozoal activity of our *N*-arylmethyl-substituted iminoribitol library (except for UAMC-00363), inhibition of the P1 and P2 transporters of *T. b. brucei* by selected compounds from this library was assessed (Table 2). The resultant K_i values, as the inhibitor concentrations that give 50% occupancy of transporter binding sites, reflect the affinity of each compound for the transporter being studied but do not necessarily correlate to uptake rates for the inhibitors. For both the P1 and P2 transporters, recognition motifs have been identified. The P1 transporters have been shown previously to interact with the substrate through hydrogen bonds at positions 3, 7, 3′, and 5′ of adenosine (2), whereas P2 binds principally with the (N-1)=(C-6)-NH$_2$ amidine motif; in addition to interactions with N-9 of the aromatic ring (Fig. 5A), the aromaticity of the purine ring itself further contributes to P2 binding (10, 14). The P2 motif is shared with the diamidines and melaminophenyl arsenicals (Fig. 5B) and has been grafted onto inhibitors as means of delivery to the cell (3, 9). On the other hand, resistance against these compounds is developed by deletion of P2 without loss of viability of the parasite (15, 28). Based on

the P2 recognition motif, compounds UAMC-00375 and UAMC-00363 (Fig. 2) were considered for affinity testing with the P2 transporter, but compounds UAMC-00109, UAMC-00311, and UAMC-00312, lacking the P2 motif, were not tested against this transporter. The respective transporter affinities were consistent with the predictions based on the known motifs and formed a rationale for the activities of the compounds based on cellular penetration. Interestingly, only inhibitor UAMC-00363 showed significant affinity toward the P2 transporter (K_i = 8.2 μM) (Fig. 6A). Its bioisostere UAMC-00375 showed 15-fold-lower affinity (K_i = 125 μM), thereby indicating that the protonated N-7 of UAMC-00363 is crucial for interactions with this class of purine analogues; in adenosine and adenine, this residue is not protonated and in this state does not appreciably contribute to binding. The low affinity of UAMC-00363 toward P1 (K_i = 355 μM) (Fig. 6B) was predictable since the 3′- and 5′-hydroxyl groups of the ribose moiety contribute strongly to P1 binding and, indeed, constitute the basis for the absolute selectivity of P1 for nucleosides over nucleobases. The orientation of the ribose ring in the P1 binding pocket is therefore critical, and the iminoribitol orientation is substantially altered, not least because of the methylene linker. For P2 binding, the ribose orientation is less strict since binding occurs mainly via the purine ring (14). An *in silico* model of P2-substrate interactions, developed using comparative molecular field analysis (CoMFA) and comparative molecular similarity indices anal-
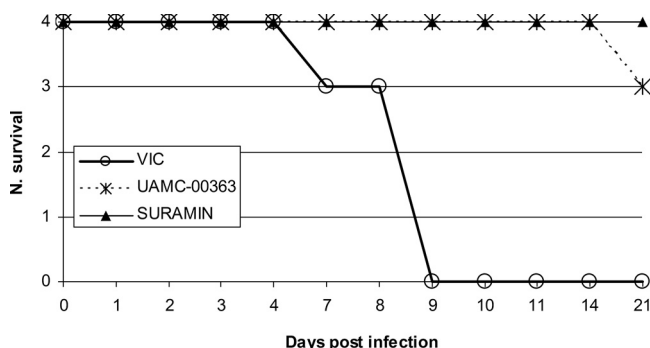

FIG. 4. Kaplan-Meier survival curves from the *in vivo* assay. Untreated mice (vehicle-infected controls [VIC]), UAMC-00363-treated mice, and suramin-treated mice were monitored for 21 dpi. Four mice were included in each group. N. survival, number of surviving mice.

TABLE 2. K_i values of NH inhibitors for the *T. b. brucei* P1, P2, and H2 transporters[a]

Compound	K_i (μM) for:		
	P1	P2	H2
UAMC-00109	>1,000	ND	ND
UAMC-00311	810 ± 220	ND	ND
UAMC-00312	300 ± 80	ND	ND
UAMC-00363	360 ± 30	8.2 ± 0.6	590
UAMC-00375	540 ± 120	125 ± 13	ND

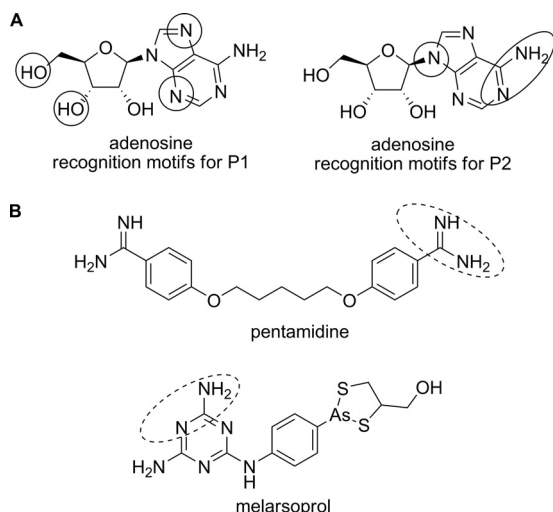[a] ND, not determined. Values are means ± standard errors.

FIG. 5. (A) Graphic representation of the recognition motifs for the P1 and P2 transporters on adenosine. (B) Structures of pentamidine and melarsoprol; the amidine motifs are circled with dashed lines.

ysis (CoMSIA) (10), showed that a positive charge at position 7 and either a hydrogen bond acceptor or donor are favored; furthermore, the computational analysis identified no steric barriers to the protonation of N-7. The combination of these factors sufficiently explained the relatively low affinity of UAMC-00375 toward P2. In addition to the nucleoside transporters, we tested the H2 hypoxanthine transporter for inhibition by UAMC-00363, as this nucleobase transporter also displays some affinity for adenosine (K_i = 590 μM) (13). UAMC-00363 did affect H2-mediated hypoxanthine uptake similarly to adenosine (Fig. 6C), but it is unlikely that this low-affinity flux significantly contributes to UAMC-00363 uptake at submicromolar concentrations. Since UAMC-00363 showed great selectivity toward *T. b. brucei* and *T. b. rhodesiense* (it was inactive against *L. infantum*, *T. cruzi*, and *P. falciparum*) and was the only compound of the series to display high affinity for any of the *T. b. brucei* purine transporters, it is temping to assume that its selective activity is dependent on accumulation through the *T. b. brucei*-specific P2 transporter. This model would predict loss of activity for the compound in

a *T. b. brucei* line not expressing P2. Therefore, both UAMC-00363 and UAMC-00375 were tested with the TbAT1-KO clonal line (derived from strain 427 but with the gene coding for TbAT1/P2 experimentally deleted [28]) and the B48 line (generated from TbAT1-KO by *in vitro* adaptation to pentamidine) (6). These lines are strongly resistant to diminazene and to all diamidines and melaminophenyl arsenicals, respectively (6, 28). Interestingly, no resistance to this compound was observed, and no cross-resistance to the amidines or the melaminophenyl arsenical compounds was observed. We conclude that UAMC-00363 enters the cell via at least one other transporter besides P2 or via passive membrane permeability, although the latter possibility is unlikely. The data summarized in Table 2 suggest that this other transport mechanism would not be one of the known *T. b. brucei* purine transporters. It can therefore not be excluded that the other inhibitors may also be taken up by the cell via this unidentified transport mechanism and that their lack of uptake by P1 or P2 is not the only reason for the absence of antiparasitic activity.

If the main target of UAMC-00363 is the NH, it would be expected that the cells would be more sensitive to the compound when provided with inosine as the sole purine source than when provided with hypoxanthine. We thus determined the IC$_{50}$s of UAMC-00363 for *T. b. brucei* strain 427 after several passages in medium that contained either hypoxanthine or inosine at a 0.1 or 1 mM concentration. We found no clear differences in the IC$_{50}$ values under the various conditions (data not shown), indicating the existence of an additional target.

RNAi knockdown. Since the purine salvage machinery is remarkably versatile because of the existence of multiple NH and phosphoribosyltransferases (PRTs) and the possibility of bypass via MTAP (Fig. 1), we chose to target the two NH of *T. b. brucei*, IAG-NH (GeneDB accession no. Tb927.3.2960) and IG-NH (GeneDB accession no. Tb927.7.4570), as well as the MTAP (GeneDB accession no. Tb927.7.7040). MTAP phosphorolytically cleaves the glycosidic bond of adenine-containing nucleosides and converts 5′-methylthioadenosine (MTA) into adenine. Via this route, MTAP is involved in both the PSP and polyamine metabolism (25). By providing adenine, MTAP can circumvent IAG-NH function. Previous results of RNAi-mediated silencing already showed that *T. b. brucei*
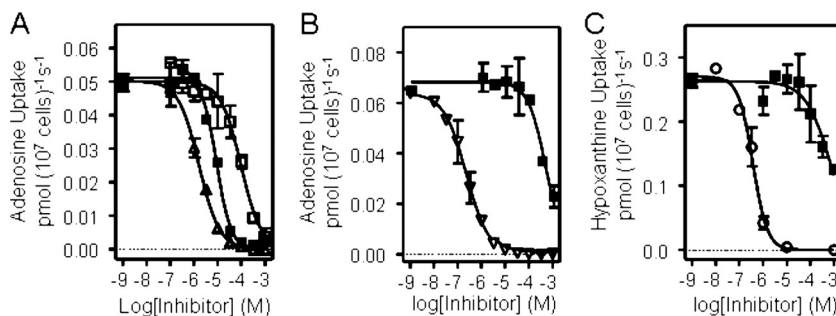

FIG. 6. Effect of UAMC-00363 on *T. b. brucei* purine transporters. Levels of purine uptake by the P2 transporter (A), the P1 transporter (B), and the H2 transporter (C) were measured using 0.05 μM [³H]adenosine in the presence of a fixed 1 mM concentration of inosine to block the P1 transporter (A), 0.05 μM [³H]adenosine in the presence of a fixed 100 μM concentration of adenine to block P2-mediated transport (B), or 0.1 μM [³H]hypoxanthine (C). Various concentrations of test compounds were added as indicated. ■, UAMC-00363; □, UAMC-00375; △, 2,6-diaminopurine 2′-deoxyriboside; ▽, adenosine; and ○, hypoxanthine. Data are the means and standard errors of the means of triplicate determinations from an experiment representative of at least three similar experiments.
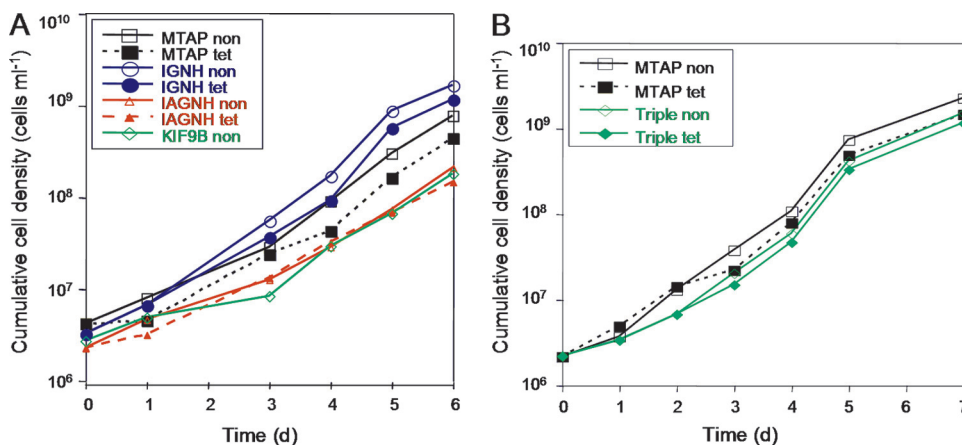
FIG. 7. (A) Growth rates of the three mutant cell lines TbIAGNH[RNAi], TbIGNH[RNAi], and TbMTAP[RNAi] (single-RNAi lines) monitored over 6 days. An uninduced control cell line, TbKIF9B[RNAi] (18), was used. non, no induction; tet, induction of RNAi with tetracycline; d, days. (B) Growth rates of the TbMTAP[RNAi] (single-RNAi) and TbMTAP-IAGNH-IGNH[RNAi] (triple-RNAi) mutant cell lines monitored over 7 days. The cumulative cell density data take into account the dilution factors of the cells during the experiment. For each mutant, the experiment was repeated with a second transfectant and similar results were obtained.

AK, responsible for the phosphorylation of adenosine to form the 5′-monophosphate AMP, is nonessential under standard growth conditions (26). PRTs were not targeted since multiple PRT genes exist and cross RNAi in an RNAi experiment could not be avoided. The expression of each enzyme was knocked down separately by RNAi, and then all three were targeted together (in a triple-RNAi analysis). The efficiency of RNAi was measured by RT-PCR, and results showed a significant reduction in total mRNA in all three cases (51.0% for IAG-NH, 64.1% for IG-NH, and 83.5% for MTAP).

Protein expression could not be measured since no antibody against NH or MTAP was available at the time. The effect of protein knockdown was evaluated by growth curve analysis, which showed a slight slowdown in the growth of TbMTAP[RNAi] and TbIGNH[RNAi] cells after 4 to 5 days of RNAi induction compared to the growth of uninduced controls (Fig. 7A). No reduction in the growth of TbIAGNH[RNAi] cells was seen, even after 6 days of induction. Although the reduction in cell growth upon the induction of RNAi was very limited, we observed abnormal cell types (multinucleate and anucleate cells) (Fig. 8) in induced TbMTAP[RNAi] cultures, indicating problems in the cell cycle and cytokinesis. These abnormal cells increased in number during the course of induction.

Since it is possible that the different enzymes complement one another, we constructed and analyzed a triple-RNAi cell line, TbMTAP-IAGNH-IGNH[RNAi]. Upon induction, this triple-RNAi cell line displayed a phenotype similar to that of cells with single IG-NH or MTAP knockdown: a slight slowdown in growth (Fig. 7B), accompanied by the appearance of abnormal cells (similar to TbMTAP[RNAi] cells) (Fig. 8), which increased in importance during longer induction periods (data not shown).

DISCUSSION

Extensive and interdisciplinary research was performed to clarify the lack of biological activity of the potent N-arylmethyl-

substituted iminoribitols (except UAMC-00363). The UAMC-00363 compound is a nanomolar inhibitor of the IAG-NH proteins from both T. vivax and T. b. brucei. However, other compounds that were previously shown to have nanomolar K_is for TvIAG-NH (4, 22, 23) are less efficient in inhibiting the T. b. brucei enzyme. These findings clearly suggest that the two enzymes, despite sharing the same substrate specificity, differ at specific amino acid residues that interact with the inhibitors. Moreover, compounds with nanomolar inhibitor constants for TbbIAG-NH are less potent ($\sim 10^{-3}$-fold as strong) against the IG-NH isozyme, underscoring the existence of distinct active site features in the two enzymes. The fact that these compounds do not sufficiently inhibit the IG-NH of T. b. brucei may be a first indication for their lack of biological activity against this parasite. In addition, it was shown that uptake of these inhibitors, except for UAMC-00363, does not happen via the P1/P2 transport system of T. b. brucei. It cannot be excluded that uptake happens via at least one other transporter, as demonstrated for UAMC-00363. RNAi results showed that procyclic T. b. brucei could survive when an NH (IAG-NH or IG-NH) had been partially knocked down (by 51 or 64%). There are two possible explanations for this observation: either the enzymes are nonessential under our experimental conditions, or there is sufficient mRNA present after tetracycline induction to sustain normal cell growth (41). Knockdown of IG-NH and MTAP has a more pronounced effect than knockdown of IAG-NH, without being lethal, although the difference is minor (again under the conditions used here). These observations are confirmed by the results of the triple-RNAi experiment. An explanation for this effect may be that MTAP is involved in, besides the PSP, polyamine biosynthesis (25). Inhibition of this enzyme may therefore have greater consequences for the parasite. The fact that the effect of IG-NH knockdown is more pronounced than that of IAG-NH knockdown can be explained by the kinetic constants of both enzymes. They suggest that IG-NH is the major NH in the PSP and that, therefore, knockdown of this enzyme will have a greater, although not lethal, effect than knockdown of
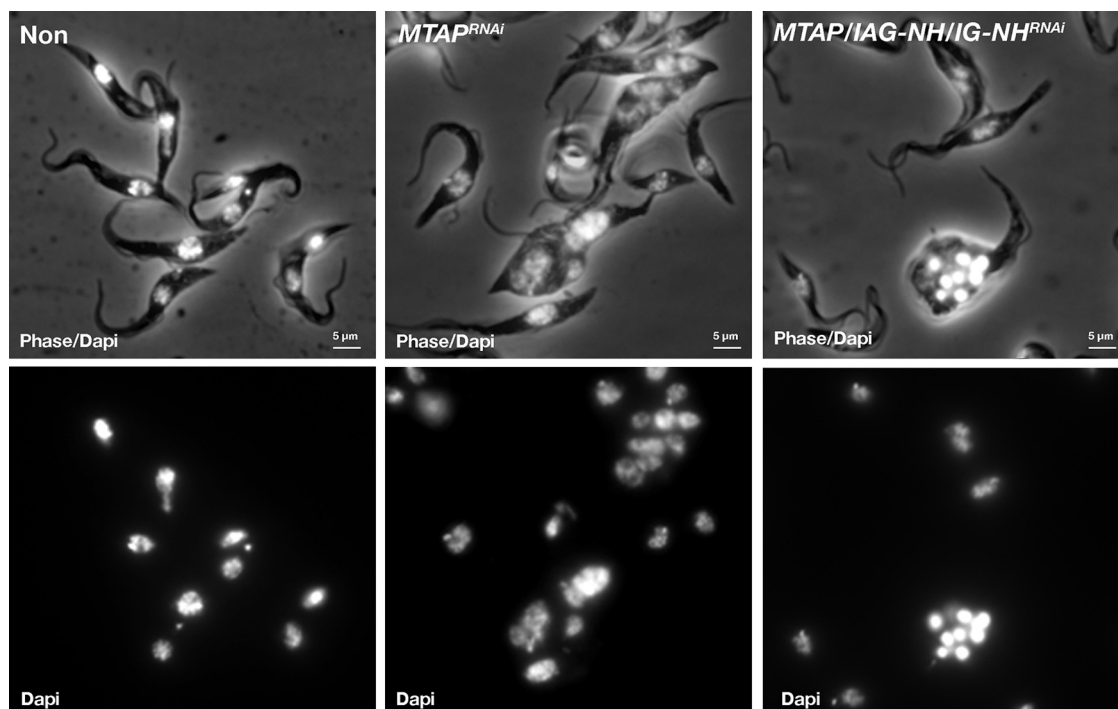
FIG. 8. Fluorescence analyses of uninduced 29-13 cells (non) (left) and induced TbMTAP^{RNAi} (middle) and TbMTAP-IAGNH-IGNH^{RNAi} (right) mutant cell lines. The top panels show combined phase-contrast/DAPI (4′,6-diamidino-2-phenylindole) images illustrating cell shape as well as DNA staining. The bottom panels illustrate the DAPI staining of the nuclei and kinetoplasts.

IAG-NH (IG-NH from *T. b. brucei* has a 10-fold-greater k_{cat}/K_m ratio than TvIAG-NH for the inosine substrate [M. Degano, unpublished results]). Although preliminary, these results are consistent with the lack of antiparasitic activity observed for our NH inhibitors. Only inhibitor UAMC-00363 shows remarkable biochemical and biological activities. It is a nanomolar inhibitor of both TvIAG-NH and TbbIAG-NH, discriminating against hPNP and TbbIG-NH. It shows selective antiparasitic activity against *T. b. brucei* and *T. b. rhodesiense* and was further characterized as having an initially trypanostatic effect, becoming rapidly trypanocidal only at high concentrations (>5 μM). While treatment with low concentrations of UAMC-00363 clears trypanosome populations only slowly (over >48 h), we demonstrated that the inhibitor triggers an irreversible process in the parasite within 5 h of incubation, after which the drug can be removed. This process appears to act rapidly to block cell division and growth, leading eventually to cell death, and is reminiscent of observations with inhibitors of *T. b. brucei* phosphodiesterases, which induce a rapid rise in the concentration of the second messenger cyclic AMP (M. K. Gould and H. P. de Koning, unpublished results). The irreversibility of effects from a brief exposure to UAMC-00363 is potentially of great therapeutic advantage, allowing shorter treatment, which in turn reduces the risk of side effects. Results of *in vivo* studies with a rodent model show complete clearance of parasites from the blood by 10 dpi and a rodent survival rate of 75% at 21 dpi. UAMC-00363 is concentrated into the cell via P2 and at least one other transporter. Interestingly, no resistance to UAMC-00363 is observed, and thus no cross-resistance to the amidines or the melaminophenyl arsenical compounds is expected. As resistance to melarsoprol and to diamidines such as diminazene has become a severe problem in the treatment of human and veterinary trypanosomiasis, the efficacy of any new compound against resistant strains is a prerequisite for its clinical consideration (17). We conclude that, among a series of 52 *N*-arylmethyl-substituted iminoribitols, UAMC-00363 shows interesting *in vitro* and *in vivo* activities against *T. b. brucei*. This compound is taken up into the parasite by the P2 transporter and at least one other transport mechanism. Besides its inhibition of IAG-NH, its antiparasitic activity is associated with other, unknown targets. It has excellent selectivity with respect to hPNP, and the parasites show no cross-resistance with respect to existing trypanocidal drugs. We believe that single inhibition of TbbIAG-NH is insufficient and that inhibition of multiple enzymes of the PSP is a prerequisite to obtain a trypanocidal effect. Further *in vivo* studies and optimization of UAMC-00363 are planned.

A. Matheeussen performed the technical laboratory work for the *in vitro* assay. The excellent technical assistance of W. Bollaert was greatly appreciated.

1. **Absalon, S., L. Kohl, C. Branche, T. Blisnick, G. Toutirais, F. Rusconi, J. Cosson, Bonhivers, D. Robinson, and P. Bastin.** 2007. Basal body positioning is controlled by flagellum formation in *Trypanosoma brucei*. PLoS One **2:**e437.
2. **Al-Salabi, M. I., L. J. M. Wallace, A. Lüscher, P. Mäser, D. Candlish, B. Rodenko, M. K. Gould, I. Jabeen, S. N. Ajith, and H. P. de Koning.** 2007. Molecular interactions underlying the unusually high adenosine affinity of a novel *Trypanosoma brucei* nucleoside transporter. Mol. Pharmacol. **71:**921–929.
3. **Barrett, M. P., and I. H. Gilbert.** 2006. Targeting of toxic compounds to the trypanosome's interior. Adv. Parasitol. **63:**125–183.
4. **Berg, M., G. Bal, A. Goeminne, P. Van der Veken, W. Versées, J. Steyaert, A. Haemers, and K. Augustyns.** 2009. Synthesis of bicyclic *N*-arylmethyl substituted iminoribitol derivatives as selective nucleoside hydrolase inhibitors. ChemMedChem **4:**249–260.
5. **Berriman, M., E. Ghedin, C. Hertz-Fowler, G. Blandin, H. Renauld, D. C. Bartholomeu, N. J. Lennard, E. Caler, N. E. Hamlin, B. Haas, U. Boehme, L. Hannick, M. A. Aslett, J. M. L. Shallom, L. Hou, B. Wickstead, U. C. M. Alsmark, C. Arrowsmith, R. J. Atkin, A. J. Barron, F. Bringaud, K. Brooks, M. Carrington, I. Cherevach, T.-J. Chillingworth, C. Churcher, L. N. Clark, C. H. Corton, A. Cronin, R. M. Davies, J. Doggett, A. Djikeng, T. Feldblyum, M. C. Field, A. Fraser, I. Goodhead, Z. Hance, D. Harper, B. R. Harris, H. Hauser, J. Hostetler, A. Ivens, K. Jagels, D. Johnson, J. Johnson, K. Jones, A. X. Kerhornou, H. Koo, N. Larke, S. Landfear, C. Larkin, V. Leech, A. Line, A. Lord, A. MacLeod, P. J. Mooney, S. Moule, D. M. A. Martin, G. W. Morgan, K. Mungall, H. Norbertczak, D. Ormond, G. Pai, C. S. Peacock, J. Peterson, M. A. Quail, E. Rabbinowitsch, M.-A. Rajandream, C. Reitter, S. L. Salzberg, M. Sanders, S. Schobel, S. Sharp, M. Simmonds, A. J. Simpson, L. Tallon, C. Turner, R. Michael, A. Tait, A. R. Tivey, S. Van Aken, D. Walker, D. Wanless, S. Wang, B. White, O. White, S. Whitehead, J. Woodward, J. Wortman, M. D. Adams, T. M. Embley, K. Gull, E. Ullu, J. D. Barry, H. Fairlamb, F. Opperdoes, B. G. Barrell, J. E. Donelson, N. Hall, C. M. Fraser, S. E. Melville, and N. M. El-Sayed.** 2005. The genome of the African trypanosome *Trypanosoma brucei*. Science **309:**416–422.
6. **Bridges, D., M. K. Gould, B. Nerima, P. Mäser, R. J. S. Burchmore, and H. P. de Koning.** 2007. Loss of the high affinity pentamidine transporter is responsible for high levels of cross-resistance between arsenical and diamidine drugs in African trypanosomes. Mol. Pharmacol. **71:**1098–1108.
7. **Carter, N. S., and A. H. Fairlamb.** 1993. Arsenical-resistant trypanosomes lack an unusual adenosine transporter. Nature **361:**173–176.
8. **Cheng, Y.-C., and W. H. Prusoff.** 1973. Relationship between the inhibition constant (K_i) and the concentration of inhibitor which causes 50 per cent inhibition (IC_{50}) of an enzymatic reaction. Biochem. Pharmacol. **22:**3099–3108.
9. **Chollet, C., A. Baliani, P. E. Wong, M. P. Barrett, and I. H. Gilbert.** 2009. Targeted delivery of compounds to *Trypanosoma brucei* using the melamine motif. Bioorg. Med. Chem. **17:**2512–2523.
10. **Collar, C. J., M. I. Al-Salabi, M. L. Stewart, M. P. Barrett, W. D. Wilson, and H. P. de Koning.** 2009. Predictive computational models of substrate binding by a nucleoside transporter. J. Biol. Chem. **284:**34028–34035. doi:10.1074/jbc.M109.049726.
11. **Cos, P., A. J. Vlietinck, D. Vanden Berghe, and L. Maes.** 2006. Demonstration of anti-infective potential of natural products—how to develop a stronger in vitro 'proof-of-concept'. J. Ethnopharmacol. **106:**290–302.
12. **de Koning, H. P., D. J. Bridges, and R. J. S. Burchmore.** 2005. Purine and pyrimidine transport in pathogenic protozoa: from biology to therapy. FEMS Microbiol. Rev. **29:**987–1020.
13. **de Koning, H. P., and S. M. Jarvis.** 1997. Purine nucleobase transport in bloodstream forms of *Trypanosoma brucei brucei* is mediated by two novel transporters. Mol. Biochem. Parasitol. **89:**245–258.
14. **de Koning, H. P., and S. M. Jarvis.** 1999. Adenosine transporters in bloodstream forms of *Trypanosoma brucei brucei*: substrate recognition motifs and affinity for trypanocidal drugs. Mol. Pharmacol. **56:**1162–1170.
15. **de Koning, H. P., M. Stewart, L. Anderson, R. Burchmore, L. J. M. Wallace, and M. P. Barrett.** 2004. The trypanocide diminazene aceturate is accumulated predominantly through the TbAT1 purine transporter: additional insights in diamidine resistance in African trypanosomes. Antimicrob. Agents Chemother. **48:**1515–1519.
16. **de Koning, H. P., C. J. Watson, and S. M. Jarvis.** 1998. Characterisation of a nucleoside/proton symporter in procyclic *Trypanosoma brucei brucei*. J. Biol. Chem. **273:**9486–9494.
17. **Delespaux, V., and H. P. de Koning.** 2007. Drugs and drug resistance in African trypanosomiasis. Drug Resist. Updat. **10:**30–50.
18. **Demonchy, R., T. Blisnick, C. Deprez, G. Toutirais, C. Loussert, W. Marande, P. Grellier, P. Bastin, and L. Kohl.** 2009. Kinesin 9 family members perform separate functions in the trypanosome flagellum. J. Cell Biol. **187:**615–622.
19. **El Kouni, M. H.** 2003. Potential chemotherapeutic targets in purine metabolism of parasites. Pharmacol. Ther. **99:**283–309.
20. **Evans, G. B., R. H. Furneaux, G. J. Gainsford, V. L. Schramm, and P. C. Tyler.** 2000. Synthesis of transition state analogue inhibitors for purine nucleoside phosphorylase and *N*-riboside hydrolases. Tetrahedron **56:**3053–3062.
21. **Evans, G. B., R. H. Furneaux, A. Lewandowicz, V. L. Schramm, and P. C. Tyler.** 2003. Synthesis of second-generation transition state analogues of human purine nucleoside phosphorylase. J. Med. Chem. **46:**5271–5276.
22. **Goeminne, A., M. Berg, M. McNaughton, G. Bal, G. Surpateanu, P. Van der Veken, S. De Prol, W. Versées, J. Steyaert, A. Haemers, and K. Augustyns.** 2008. *N*-Arylmethyl substituted iminoribitol derivatives as inhibitors of a purine specific nucleoside hydrolase. Bioorg. Med. Chem. **16:**6752–6763.
23. **Goeminne, A., M. McNaughton, G. Bal, G. Surpateanu, P. Van der Veken, S. De Prol, W. Versées, J. Steyaert, A. Haemers, and K. Augustyns.** 2008. Synthesis and biochemical evaluation of guanidine-alkyl-ribitol derivatives as nucleoside hydrolase inhibitors. Eur. J. Med. Chem. **43:**315–326.
24. **Kicska, G. A., P. C. Tyler, G. B. Evans, R. H. Furneaux, V. L. Schramm, and K. Kim.** 2002. Purine-less death in *Plasmodium falciparum* induced by Immucilin-H, a transition state analogue of purine nucleoside phosphorylase. J. Biol. Chem. **277:**3226–3231.
25. **Lawton, P.** 2005. Purine analogues as antiparasitic agents. Expert Opin. Ther. Pat. **15(8):**987–994.
26. **Lüscher, A., P. Önal, A. M. Schweingruber, and P. Mäser.** 2007. Adenosine kinase of *Trypanosoma brucei* and its role in susceptibility to adenosine antimetabolites. Antimicrob. Agents Chemother. **51:**3895–3901.
27. **Mäser, P., C. Sutterlin, A. Kralli, and R. Kaminsky.** 1999. A nucleoside transporter from *Trypanosoma brucei* involved in drug resistance. Science **285:**242–244.
28. **Matovu, E., M. Stewart, F. Geiser, R. Brun, P. Mäser, L. J. M. Wallace, R. J. Burchmore, J. C. K. Enyaru, M. P. Barrett, R. Kaminsky, T. Seebeck, and H. P. de Koning.** 2003. The mechanisms of arsenical and diamidine uptake and resistance in *Trypanosoma brucei*. Eukaryot. Cell **2:**1003–1008.
29. **Miles, R. W., P. C. Tyler, G. B. Evans, R. H. Furneaux, D. W. Parkin, and V. L. Schramm.** 1999. Iminoribitol transition state analogue inhibitors of protozoan nucleoside hydrolases. Biochemistry **38:**13147–13154.
30. **Muzzolini, L., W. Versées, P. Tornaghi, E. Van Holsbeke, J. Steyaert, and M. Degano.** 2006. New insights into the mechanism of nucleoside hydrolases from the crystal structure of the *Escherichia coli* YbeK protein bound to the reaction product. Biochemistry **45:**773–782.
31. **Ortiz, D., M. A. Sanchez, P. Quecke, and S. M. Landfear.** 2009. Two novel nucleobase/pentamidine transporters from *Trypanosoma brucei*. Mol. Biochem. Parasitol. **163:**67–76.
32. **Parkin, D. W.** 1996. Purine-specific nucleoside *N*-ribohydrolase from *Trypanosoma brucei brucei*. Purification, specificity, and kinetic mechanism. J. Biol. Chem. **271:**21713–21719.
33. **Pellé, R., V. L. Schramm, and D. W. Parkin.** 1998. Molecular cloning and expression of a purine-specific *N*-ribohydrolase from *Trypanosoma brucei brucei*. Sequence, expression, and molecular analysis. J. Biol. Chem. **273:**2118–2126.
34. **Rodenko, B., A. M. van der Burg, M. J. Wanner, M. Kaiser, R. Brun, M. Gould, H. P. de Koning, and G.-J. Koomen.** 2007. 2,N^6-Disubstituted adenosine analogues with antitrypanosomal and antimalarial activities. Antimicrob. Agents Chemother. **51:**3796–3802.
35. **Sanchez, M. A., R. Tryon, J. Green, I. Boor, and S. M. Landfear.** 2002. Six related nucleoside/nucleobase transporters from *Trypanosoma brucei* exhibit distinct biochemical functions. J. Biol. Chem. **277:**21499–21504.
36. **Ullman, B., and D. Carter.** 1997. Molecular and biochemical studies on the hypoxanthine-guanine phosphoribosyltransferases of the pathogenic haemoflagellates. Int. J. Parasitol. **27:**203–213.
37. **Versées, W., J. Barlow, and J. Steyaert.** 2006. Transition-state complex of the purine-specific nucleoside hydrolase of *T. vivax*: enzyme conformational changes and implications for catalysis. J. Mol. Biol. **359:**331–346.
38. **Versées, W., K. Decanniere, R. Pellé, J. Depoorter, E. Brosens, D. W. Parkin, and J. Steyaert.** 2001. Structure and function of a novel purine specific nucleoside hydrolase from *Trypanosoma vivax*. J. Mol. Biol. **307:**1363–1379.
39. **Versées, W., A. Goeminne, M. Berg, A. Vandemeulebroucke, A. Haemers, K. Augustyns, and J. Steyaert.** 2009. Crystal structures of *T. vivax* nucleoside hydrolase in complex with new potent and specific inhibitors. Biochim. Biophys. Acta **1794(6):**953–960.
40. **Wallace, L. J. M., D. Candlish, and H. P. De Koning.** 2002. Different substrate recognition motifs of human and trypanosome nucleobase transporters: selective uptake of purine antimetabolites. J. Biol. Chem. **277:**26149–26156.
41. **Wang, Z., J. C. Morris, M. E. Drew, and P. T. Englund.** 2000. Inhibition of *Trypanosoma brucei* gene expression by RNA interference using an integratable vector with opposing T7 promoters. J. Biol. Chem. **275:**40174–40179.
42. **Wirtz, E., S. Leal, C. Ochatt, and G. A. M. Cross.** 1999. A tightly regulated inducible expression system for conditional gene knock-outs and dominant-negative genetics in *Trypanosoma brucei*. Mol. Biochem. Parasitol. **99:**89–101.
43. **Zamudio, J. R., B. Mittra, A. Chattopadhyay, J. A. Wohlschlegel, N. R. Sturm, and D. A. Campbell.** 2009. *Trypanosoma brucei* spliced leader RNA maturation by the cap 1 2′-*O*-ribose methyltransferase and SLA1 H/ACA snoRNA pseudouridine synthase complex. Mol. Cell. Biol. **29:**1202–1211.